

# Long-term correction of ornithine transcarbamylase deficiency in Spf-Ash mice with a translationally optimized AAV vector

Giulia De Sabbata,<sup>1</sup> Florence Boisgerault,<sup>2,3</sup> Corrado Guarnaccia,<sup>1</sup> Alessandra Iaconig,<sup>1</sup> Giulia Bortolussi,<sup>1</sup> Fanny Collaud,<sup>2,3</sup> Giuseppe Ronzitti,<sup>2,3</sup> Marcelo Simon Sola,<sup>2,3</sup> Patrice Vidal,<sup>2,3</sup> Jeremy Rouillon,<sup>2,3</sup> Severine Charles,<sup>2,3</sup> Emanuele Nicastrò,<sup>4</sup> Lorenzo D'Antiga,<sup>4</sup> Petr Ilyinskii,<sup>5</sup> Federico Mingozzi,<sup>2,3,6</sup> Takashi Kei Kishimoto,<sup>5</sup> and Andrés F. Muro<sup>1</sup>

<sup>1</sup>International Center for Genetic Engineering and Biotechnology (ICGEB), 34149 Trieste, Italy; <sup>2</sup>Généthon, 91000 Evry, France; <sup>3</sup>Université Paris-Saclay, Université Evry, INSERM, Généthon, Intégrare Research Unit UMR\_S951, 91000 Evry, France; <sup>4</sup>Ospedale Papa Giovanni XXIII, 24127 Bergamo, BG, Italy; <sup>5</sup>Selecta Biosciences, Watertown, MA 02472, USA; <sup>6</sup>Institut de Myologie, 73013 Paris, France

**Ornithine transcarbamylase deficiency (OTCD) is an X-linked liver disorder caused by partial or total loss of OTC enzyme activity. It is characterized by elevated plasma ammonia, leading to neurological impairments, coma, and death in the most severe cases. OTCD is managed by combining dietary restrictions, essential amino acids, and ammonia scavengers. However, to date, liver transplantation provides the best therapeutic outcome. AAV-mediated gene-replacement therapy represents a promising curative strategy. Here, we generated an AAV2/8 vector expressing a codon-optimized human OTC cDNA by the  $\alpha$ 1-AAT liver-specific promoter. Unlike standard codon-optimization approaches, we performed multiple codon-optimization rounds via common algorithms and ortholog sequence analysis that significantly improved mRNA translatability and therapeutic efficacy. AAV8-hOTC-CO (codon optimized) vector injection into adult OTC<sup>Spf-Ash</sup> mice (5.0E11 vg/kg) mediated long-term complete correction of the phenotype. Adeno-Associated viral (AAV) vector treatment restored the physiological ammonia detoxification liver function, as indicated by urinary orotic acid normalization and by conferring full protection against an ammonia challenge. Removal of liver-specific transcription factor binding sites from the AAV backbone did not affect gene expression levels, with a potential improvement in safety. These results demonstrate that AAV8-hOTC-CO gene transfer is safe and results in sustained correction of OTCD in mice, supporting the translation of this approach to the clinic.**

## INTRODUCTION

Inherited metabolic disorders affecting the urea cycle can trigger severe hyperammonemia, with the risk of permanent cognitive impairment, coma, and death.<sup>1</sup> Urea cycle disorders account for about 1 every 8,000 births worldwide.<sup>2,3</sup> Ornithine transcarbamylase deficiency (OTCD) is the most common cause of urea cycle disorders, with a worldwide incidence estimated between 1:17,000 to 1:60,000 live births.<sup>4,5</sup> Mutations in the X-linked *OTC* gene reduce or ablate OTC

function, resulting in the impairment of urea production and accumulation of neurotoxic ammonium, glutamine, and other amino acids, and increased excretion of urinary orotic acid. Complete deficiency of OTC results in the most severe form of the disease, which presents in the first days of life and is associated with permanent neurological impairment and high mortality.<sup>6</sup> In milder forms, the symptoms may manifest later in life, with altered neurocognitive status, reduced consciousness, and lethargy. OTCD can be managed with a low-protein diet combined with ammonia scavengers, which activate alternative nitrogen clearance pathways, but does not prevent hyperammonemic crises.<sup>6,7</sup> The only curative treatment for OTCD is liver transplantation, a procedure that may have substantial morbidity and mortality, is limited by the availability of compatible donor organs, and requires life-long immunosuppression to avoid organ rejection.<sup>8–10</sup>

Liver-directed gene therapy mediated by recombinant adeno-associated viral (rAAV) vectors holds great promise in treating adult patients suffering from monogenic diseases of the liver.<sup>11–14</sup> The potential of adeno-associated virus (AAV)-based gene therapy to correct the OTCD phenotype has been demonstrated in the OTC<sup>Spf-Ash</sup> mouse model,<sup>15–18</sup> but a clinically approved gene-therapy product to treat OTCD is still lacking. AAV8 was previously demonstrated to be very efficient in liver transduction in rodents and non-human primates, with clinical trials confirming the safety of the vector.<sup>11–14</sup> However, despite the non-integrative nature of AAV, concerns about the potential insertional mutagenesis and tumorigenesis mediated by AAV vectors are a matter of debate.<sup>19–23</sup> For example, it has been recently reported that fragments of AAV wild-type (WT) genomes were found integrated in the proximity of known cancer-related genes and were possibly associated with the development of hepatocellular

Received 9 July 2020; accepted 11 November 2020;  
<https://doi.org/10.1016/j.omtm.2020.11.005>.

**Correspondence:** Andrés F. Muro, International Center for Genetic Engineering and Biotechnology (ICGEB), 34149 Trieste, TS, Italy.

**E-mail:** [muro@icgeb.org](mailto:muro@icgeb.org)



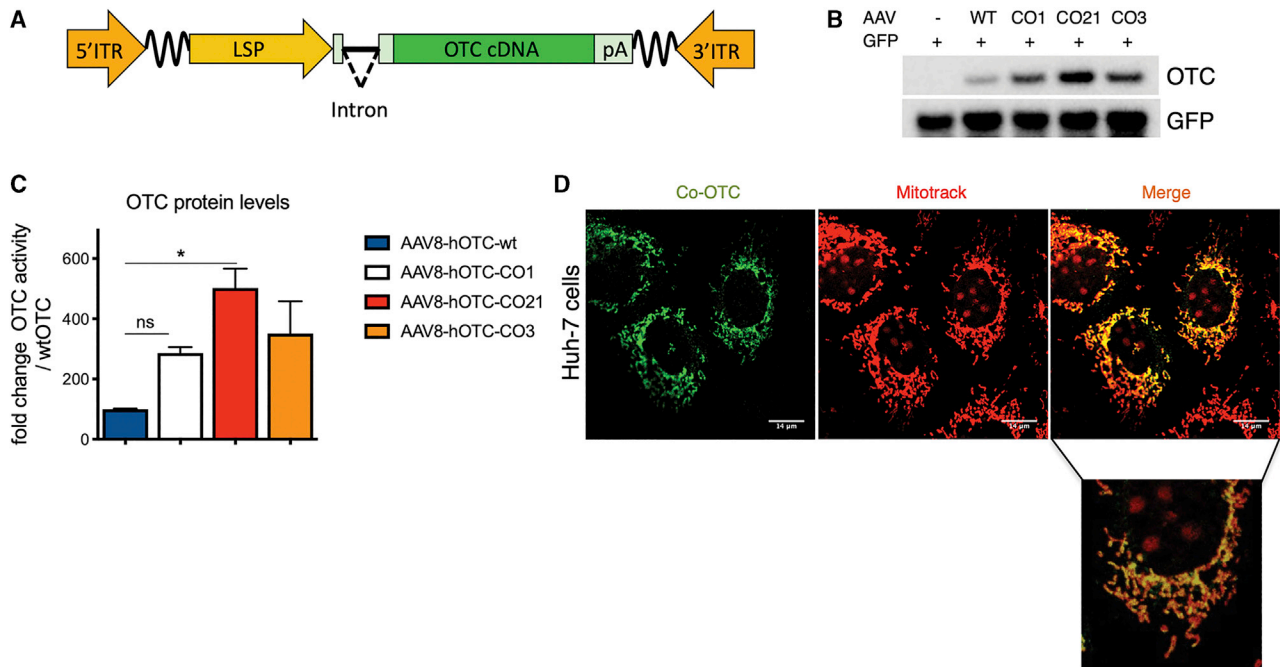


**Figure 1. Codon optimization of the hOTC cDNA increases protein production without affecting sub-cellular localization**

(A) Scheme of the rAAV-hOTC expression cassette. ITR, AAV2 inverted terminal repeat; intron, modified hemoglobin (*HBB2*) beta intron; LSP, liver-specific promoter (*ApoE/hAAT*, hybrid promoter containing *ApoE* enhancer and *hAAT* promoter); hOTC, WT or CO hOTC open reading frame (ORF); pA, hemoglobin beta (*HBB*) polyadenylation signal; the wavy lines indicate AAV backbone sequences between the expression cassette and ITRs. (B) Analysis of HCC cell line Huh-7 transfected with first group of hOTC-CO constructs. Representative western blot analysis of OTC protein levels in Huh-7 cell lysates (15 μg of protein per lane) following co-transfection of the pSMD2-hOTC-WT, pSMD2-hOTC-CO01, pSMD2-hOTC-CO21, and pSMD2-hOTC-CO03 constructs and GFP plasmids. The control lane contains cell lysate from cells transfected with the GFP-expressing plasmid. (C) Densitometric quantification of hOTC proteins from (B). GFP was used as transfection control. Values are expressed as fold change with respect to the pSMD2-hOTC-WT plasmid. Data are shown as mean ± SEM, and statistical analyses were performed by one-way ANOVA with Turkey's multiple comparison test ( $n = 2$ ,  $*p < 0.05$ ). (D) Sub-cellular localization studies of hOTC in Huh-7 human liver cells. Huh-7 cells were transfected with plasmids encoding the hOTC-CO21 variant. Mitochondria (red, MITO-TRACK) and hOTC (green) were detected with a confocal microscope. A magnified picture of the indicated area is shown below the low-resolution picture. The scale bar corresponds to 14 μm.

carcinomas (HCCs).<sup>20</sup> These sequences, located next to the AAV inverted terminal repeat (ITR) regions, contained transcription factor binding sites (TFBSs) that function as a liver-specific enhancer-promoter elements, potentially able to transactivate neighboring genes upon integration in the genome.<sup>24</sup> These observations highlight the importance of vector optimization and long-term safety assessments both in the preclinical and the clinical settings.

In the present work, we developed a therapeutic liver-specific AAV2/8 vector expressing a codon-optimized version of human *OTC* cDNA under the transcriptional control of the human alpha-1 antitrypsin (*hAAT*) promoter and apolipoprotein E (*ApoE*) enhancer<sup>25</sup>, which was highly efficient in expressing an enzymatically active OTC protein, with long-term efficacy in rescuing the diseased phenotype of *OTC*<sup>Spf-Ash</sup> mice. In contrast to standard approaches,<sup>18,26</sup> we performed multiple rounds of codon-optimization of the human *OTC* (hOTC) cDNA via common algorithms and ortholog sequence analysis to improve mRNA translatability and therapeutic efficacy. This translationally optimized candidate clinical vector, in which the ITR-associated enhancer-promoter elements were removed, presents improved safety features,

provides sustained therapeutic efficacy in *OTC*<sup>Spf-Ash</sup> mice, and therefore has the potential to achieve therapeutic efficacy in OTCD patients.

## RESULTS

### Codon optimization of human *OTC* significantly improves *in vitro* hOTC expression and activity

In order to improve the overall efficacy of the gene-therapy approach for OTCD, an initial set of codon-optimized (CO) variants of the *OTC* cDNA were generated using different optimization algorithms (CO3, CO9, CO6A, CO9-1, and CO9-2). The obtained sequences were then analyzed for the presence of potential cryptic splicing sites using splicing-specific software, which were manually removed. Potential alternative reading frames (ARFs) located in the coding and non-coding strands were also manually removed to decrease the risk of undesired cytotoxic T lymphocyte (CTL)-mediated immune responses directed against AAV-transduced hepatocytes expressing aberrant transgene products generated by ARFs, with the consequent reduction of overall efficacy.<sup>25,27</sup> The human WT hOTC cDNA and all different optimized hOTC cDNAs were cloned in the pSDMD2 vector, under the transcriptional control of the *hAAT* promoter and *ApoE* enhancer<sup>25</sup>

(liver-specific promoter [LSP]; Figure 1A). In addition, we synthesized the CO LW4 hOTC clinical candidate described by Wang et al.<sup>18</sup> and also cloned it into the pSDMD2 vector under the hAAT promoter (hOTC CO1 construct).

The resulting plasmids were transfected into the human liver cell line Huh-7 to evaluate the OTC protein expression levels (Figure 1B; Figures S1A and S1B). Western blot analysis demonstrated a variable range of protein levels, with some hOTC-CO variants showing a robust increase in the efficiency of protein production compared to the construct expressing the WT hOTC cDNA (Figures S1A and S1B; hOTC-CO1, hOTC-CO3, and hOTC-CO9).

In a second phase, we aligned the OTC amino acid sequences of 142 species (Figure S2; Table S1) to identify the conserved regions and domains containing the active site of the enzyme.<sup>28,29</sup> The alignments were manually adjusted to the human OTC primary sequence. Next, we generated additional OTC variants, hOTC-CO18 and hOTC-CO21, by shuffling the conserved domains (Figure S3) of the most active variants (hOTC-CO1, hOTC-CO3, and hOTC-CO9) from the initial phase of screening. After transient transfection in Huh-7 cells, we observed that the hOTC-CO21 version showed a 5-fold increase in protein expression levels, which was higher than the levels obtained with the original CO versions (Figures 1B and 1C; Figures S1A and S1B).

Importantly, we confirmed the correct mitochondrial import and subcellular localization of the hOTC proteins by assessing the colocalization of the exogenous hOTC proteins with the mitochondrial marker Mitotrack. As expected, all variants presented mitochondrial localization (Figure 1D; Figure S1C).

These results indicate that a combination of codon optimization and shuffling of conserved and active domain sequences is an effective strategy to derive highly expressed hOTC cDNA variants.

#### Codon optimization of human OTC cDNA significantly improves *in vivo* hOTC expression and activity

To further confirm the activity of these variants *in vivo*, AAV8-hOTC-WT, AAV8-hOTC-CO1, AAV8-hOTC-CO3, and AAV8-hOTC-CO21 were intravenously injected in adult WT mice at a dose of 5.0E12 viral genomes (vg)/kg. In line with the *in vitro* observations, hepatic expression levels and enzymatic activity were significantly increased upon treatment with the hOTC-CO1, hOTC-CO3, and hOTC-CO21 variants, compared to the hOTC-WT construct (Figures 2A–2C). Consistently, mice injected with hOTC-CO21 variant displayed a 5- to 6-fold increase in protein expression and enzyme activity compared to hOTC-WT and was significantly higher than that obtained with hOTC-CO1 and hOTC-CO3 (Figures 2A–2C). All injected animals had similar vg copy numbers (Figure 2D), suggesting that the observed differences in OTC protein levels and catalytic activity were related to the effect of different codon-optimization strategies on mRNA translation. Thus, based on *in vitro* and *in vivo* data, the variant hOTC-CO21 was identified as the most

efficient one, compared to WT and CO1 hOTC cDNAs (Figures 1B, 1C, 2A, and 2D).

Interestingly, despite having a similar expected molecular weight (MW) (39.70 kDa and 39.87 kDa, for the human and mouse OTC, respectively) and 97.73% amino acid similarity, the human OTC protein migrated slower than the mouse counterpart (Figure S4).

These findings show that the CO AAV8-hOTC-CO21 vector was the most effective in robustly driving expression of the hOTC transgene *in vivo*.

#### AAV8-hOTC CO21-mediated gene therapy restores OTC expression and urea cycle in adult OTC<sup>Spf-Ash</sup> mice

To determine the therapeutic efficacy of AAV8-hOTC-CO21, we first performed a short-term dose-finding experiment in the OTC<sup>Spf-Ash</sup> mouse model of OTCD.<sup>30,31</sup>

AAV8-hOTC-WT and AAV8-hOTC-CO21 were injected in 12-week-old OTC<sup>Spf-Ash</sup> male mice with 3 different doses: 2.5E11, 5.0E11, and 1.0E12 vg/kg. Animals were sacrificed 8 weeks after AAV delivery. The therapeutic efficacy was determined by the correction of urinary orotic acid levels, the main biomarker for OTCD. The AAV8-hOTC-WT vector restored physiological levels of urinary orotic acid at the dose of 1.0E12 vg/kg but did not correct the phenotype at lower doses (Figure 3A). In contrast, the AAV8-hOTC-CO21 vector normalized urinary orotic acid in OTC<sup>Spf-Ash</sup> mice at a lower dose (5.0E11 vg/kg) compared to the human WT version (Figures 3A and 3B). Quantification of OTC protein in the liver by western blot analysis correlated with the observed therapeutic efficacy. The levels of OTC protein of WT animals were comparable to those obtained with the highest dose of the AAV8-hOTC-WT vector (1.0E12vg/kg), while in the case of the CO21 cDNA-expressing vector, the WT levels were comparable to those of the intermediate dose (5.0E11vg/kg) (Figures 3C–3F).

To note, the AAV8-hOTC-CO21 vector was able to restore WT levels of catalytically active OTC in the liver at a dose of 5.0E11 vg/kg (Figures 3G and 3H), with an ~20-fold increase in OTC enzyme activity compared to untreated OTC<sup>Spf-Ash</sup> mice (Figure 3G).

These data show that treatment of adult OTC<sup>Spf-Ash</sup> mice with AAV8-hOTC-CO21 at a vector dose of 5.0E11 vg/kg was sufficient to express WT levels of human OTC and correct the phenotype in the short term and that the use of hOTC-CO21 CO transgene may allow for a 2-fold reduction of the therapeutic dose compared to the hOTC WT version.

Next, we assessed the ability of our therapeutic vector to restore the urea cycle in OTC<sup>Spf-Ash</sup> mice in an acute response to an ammonia challenge, a test commonly used to assess the clinical protection of the gene-therapy treatment against a provocative nitrogen acute increase.<sup>15,17,32,33</sup> A new group of adult OTC<sup>Spf-Ash</sup> mice was dosed with 5.0E11 vg/kg of AAV8-hOTC-WT or AAV8-hOTC-CO21

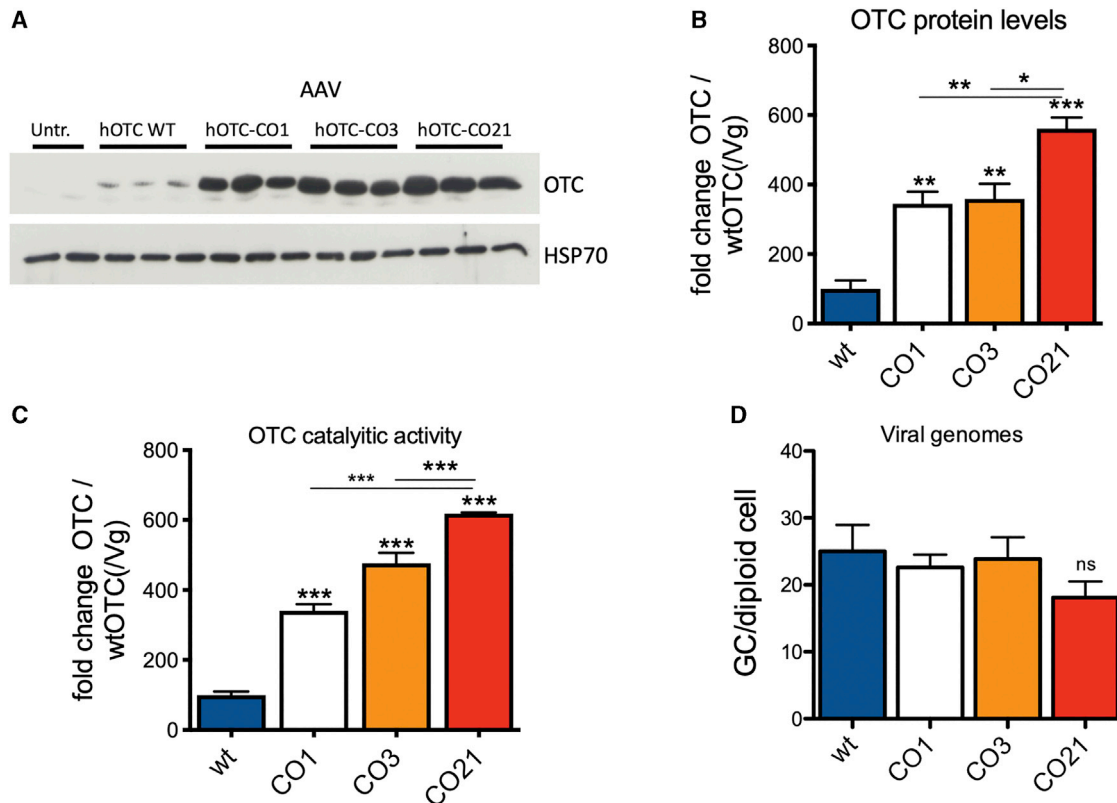


**Figure 2. Analysis of WT male mice transduced with the AAV8 hOTC constructs**

WT C57BL/6 male mice (8 weeks old) were i.v. transduced with 5.0E12 vg/kg of the indicated AAV2/8 constructs. Liver samples were collected at 14 days after viral transduction. (A) Representative WB analysis of liver extracts from control and AAV-treated animals ( $n = 3$  per construct). Samples from two untreated mice were loaded in the first two lines of the gel. The OTC and HSP70 bands are shown. In the OTC panel, the faint band presenting a slightly faster mobility than the most prominent one corresponds to the endogenous murine OTC (see Figure S4). (B) Densitometric quantification of the Western blot (WB) of (A), relative to the OTC-WT values, normalized by the vg copy number ( $n = 3$  per group). (C) OTC enzyme activity expressed in  $\mu\text{mol}$  of citrulline produced in 30 min of reaction, normalized by the vg copy number ( $n = 3$  per group). (D) Viral genome copy number quantification by quantitative real-time PCR. The mean value of two independent determinations is indicated ( $n = 3$  per group). Statistical significance compared to hOTC-WT is shown above the bar for each experimental group, and statistical significance between experimental groups is indicated by the horizontal line. (B) One-way ANOVA,  $p < 0.0001$ ; (C) one-way ANOVA,  $p < 0.0001$ ; (D) one-way ANOVA, not significant (NS); Tukey's comp. tests, \* $p < 0.05$ , \*\* $p < 0.01$ ; \*\*\* $p < 0.001$ .

(intravenously [i.v.]), and the ammonia challenge (7.5 mmol of ammonia/kg, intraperitoneally [i.p.]) was performed 4 and 8 weeks after vector dosing (Figure 4A). The efficiency of ammonia clearance was quantified 20 min after the challenge by determining plasma ammonia levels and scoring the animals for ataxia and gait abnormalities, seizures, and sound sensitivity (Figure 4B), as previously described.<sup>15,17,32,33</sup> The composite score of AAV8-hOTC-CO21-injected animals was comparable to that of untreated WT animals and AAV8-hOTC-WT-treated OTC<sup>Spf-Ash</sup> mice (Figure 4B). As expected, untreated OTC<sup>Spf-Ash</sup> mice were moribund and displayed a low behavioral score at the 4- and 8-week time points, with increased plasma ammonia levels, as a consequence of urea cycle dysfunction (Figures 4B and 4C). Treatment with either the AAV8-hOTC-WT or the AAV8-hOTC-CO21 vector successfully restored ammonia detoxification by reducing serum ammonia to physiological levels, after challenge with ammonia at both 4 weeks and 8 weeks post-gene-therapy injection (Figure 4C). These findings showed that an acute increase of ammonia in OTCD adult mice could be managed by AAV8-

hOTC-CO21 vector-driven OTC hepatic expression. Enzyme catalytic activity was much higher with the AAV8-hOTC-CO21 vector as compared to AAV8-hOTC-WT construct (Figure 4D), confirming previous results obtained with a separate group of OTC<sup>Spf-Ash</sup> animals (Figure 3G).

#### Deletion of the HCC-related liver-specific enhancer sequence in the AAV backbone did not affect the therapeutic efficacy

In an effort to improve the potential safety of the gene-therapy vector, a variant of the AAV-hOTC-CO21 vector was generated in which putative liver-specific TFBSs, which may function as a liver-specific enhancer-promoters,<sup>24</sup> were removed (AAV-hOTC-CO21 $\Delta$ Enhancer; Figure 5A) and tested side-by-side with the unmodified AAV-hOTC-CO21 vector at a dose of 1.0E12 vg/kg injected i.v. in adult OTC<sup>Spf-Ash</sup> mice. Urinary orotic acid levels were assessed every 2 weeks, and protein expression levels and vg copies were determined at sacrifice of the animals, 8 weeks after viral delivery (Figures 5B–5E). Treatment with either AAV-hOTC-CO21 or



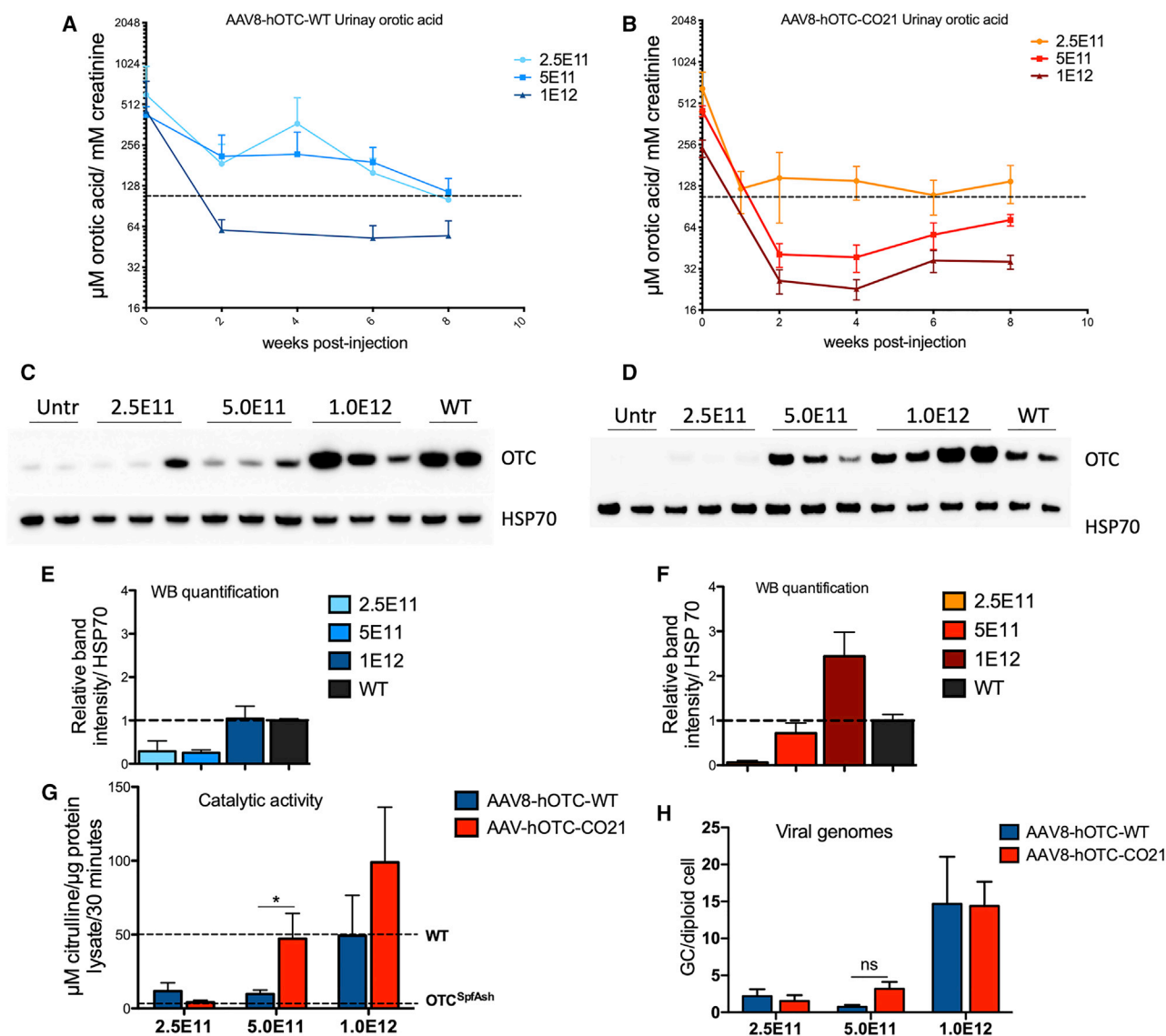


**Figure 3. Side-by-side comparison in male OTC<sup>Spf-Ash</sup> mice transduced with AAV8-hOTC-WT and AAV8-hOTC-CO21**

(A and B) 3-month-old OTC<sup>Spf-Ash</sup> mice were i.v. injected with 2.5E11 vg/kg (n = 4), 5.0E11 vg/kg (n = 5), or 1.0E12 vg/kg (n = 5) of AAV8-hOTC-WT (A) or AAV8-hOTC-CO21 (B). Mice were sacrificed 8 weeks after viral delivery. Urine samples were collected every 2 weeks post-injection and analyzed for orotic acid. The dashed line delimits the physiological level of orotic acid in WT animals. Two-way ANOVA, 5.0E11 vg/kg, AAV8-hOTC-WT versus AAV8-hOTC-CO21, p < 0.01. (C–F) OTC protein levels were determined by WB from liver extracts from AAV8-hOTC-WT (C) and AAV8-hOTC-CO21 (D). The densitometric quantification of the OTC-specific bands, normalized by the housekeeping HSP70 protein and vg copies is shown in (E) and (F). (G) OTC enzyme activity expressed in µmol of citrulline produced in 30 min of reaction. Enzyme activity of WT and OTC<sup>Spf-Ash</sup> liver extracts is indicated by the dashed lines. Data are shown as mean ± SEM, and statistical analyses were performed by one-way ANOVA with Tukey’s multiple comparison test (n = 3–5 per group; \*p < 0.05). (H) The vg particles were determined by quantitative real-time PCR, and the mean values of two independent determinations are indicated (n = 4–5 per group). Data are shown as mean ± SEM, and statistical analyses were performed by two-way ANOVA with Tukey’s multiple comparison test (\*p < 0.05).

AAV-hOTC-CO21ΔEnhancer vectors significantly decreased urinary orotic acid to normal levels, while no differences were observed between the treated groups (Figure 5B), which presented similar OTC protein levels and vg copy numbers in the liver (Figures 5C–5E). These findings indicate that the absence of the enhancer element had no significant impact in the activity of the ApoE enhancer and hAAT promoter, which drive transcription of the hOTC cDNA. Thus, for the

next series of experiments, we utilized the AAV-hOTC-CO21ΔEnhancer vector.

**AAV-hOTC-CO21ΔAV-hOTC vector drives long-term therapeutic efficacy in the mature liver**

To assess the long-term therapeutic efficacy of gene transfer in adult mice, we treated 12-week-old OTC<sup>Spf-Ash</sup> mice with 5.0E11 or 1.0E12

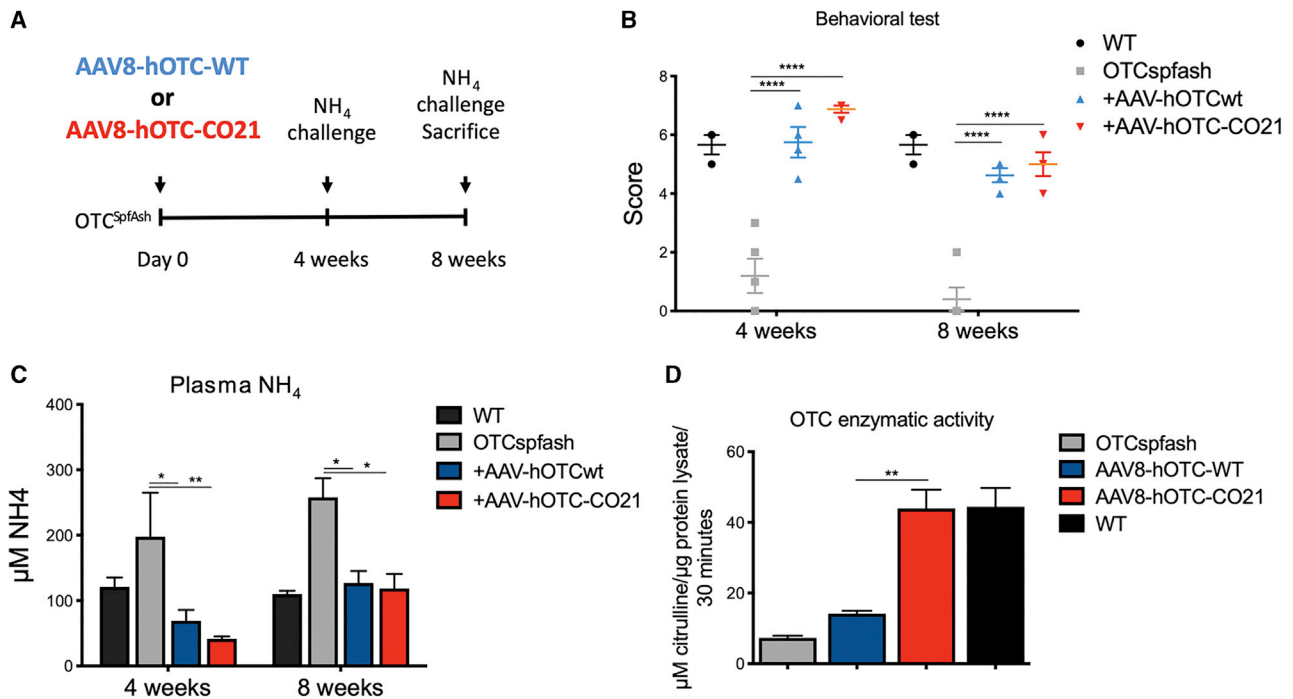


**Figure 4. Ammonia challenge of OTC<sup>Spf-Ash</sup> mice injected with 5.0E11 vg/kg of AAV8-hOTC-WT and AAV8-hOTC-CO21**

(A) Experimental scheme. 12-week-old mice were i.v. injected with 5.0E11 vg/kg of the indicated AAV8 constructs (n = 4). (B–D) Ammonia challenge was performed twice: at 4 and at 8 weeks post-injection. In each challenge, mice were evaluated with a set of behavioral tests (B), and plasma ammonia levels were determined (C). At 8 weeks post-injection, mice were sacrificed and liver was analyzed for OTC catalytic activity (D). Data are shown as mean ± SEM, and statistical analyses were performed by two-way ANOVA with Bonferroni's multiple comparison test (\*p < 0.05; \*\*p < 0.01; \*\*\*p < 0.001).

vg/kg of AAV-hOTC-CO21ΔEnhancer vector and animals were followed up for 40 weeks. Urinary orotic acid levels were monitored for the duration of the experiment, while genome copy number and OTC enzymatic activity and protein levels were determined in the liver at the sacrifice (Figure 6). In line with previous experiments, both groups of animals presented stable urinary orotic acid levels, which were within normal values for the whole duration of the experiment. As expected, we observed lower urinary orotic acid levels in the animals treated with the higher vector dose (Figure 6A). A dose effect was observed for OTC protein levels, enzymatic activity, and vg copies measured in the liver (Figures 6B–6E). These results indicate that our AAV-hOTC-CO21ΔEnhancer vector provided efficient and durable correction of OTC expression and activity in adult mice.

#### A high dose of AAV-hOTC-CO21 vector does not increase serum levels of liver transaminase

To get a deeper insight on the safety of the procedure, we injected OTC<sup>Spf-Ash</sup> mice with a dose that was 13 times higher than the therapeutic dose determined in the previous experiments (1.3E13 vg/kg), a dose similar to the high vector dose used in a current clinical trial for OTCD (ClinicalTrials.gov: NCT02991144). Urinary orotic acid and liver transaminases (aspartate aminotransferase, AST, and alanine aminotransferase, ALT) were determined at 2, 7, and 14 days after

treatment. Urinary orotic acid levels were below the normal values, while no increases over normal levels were observed in serum liver transaminases, with values similar to those of untreated mice (Figure S5).

These results provide preliminary insights on the safety and efficacy of the AAV-hOTC-CO21ΔEnhancer vector and support the potential translation of the therapeutic approach to OTCD patients.

## DISCUSSION

Liver gene therapy in hemophilia A and B clinical trials have shown safety and therapeutic potential of AAV vectors.<sup>11–14</sup> However, a metabolic disease such as OTCD presents a more challenging clinical condition for gene-replacement therapy, due to the severity of the disease. Potentially lethal hyperammonaemic episodes must be prevented in all severely affected male pediatric patients since birth, some of which are awaiting liver transplantation. In addition, about 20% of adult heterozygous females present with clinical manifestations.<sup>5</sup> The higher severity of OTCD, compared to hemophilia A and B, which require lower production of the therapeutic protein,<sup>11–14</sup> suggests that normalization of hepatic expression of OTC mediated by gene therapy may require efficient transduction of hepatocytes and elevated levels of the enzyme activity and, consequently, a highly effective gene-replacement vector.

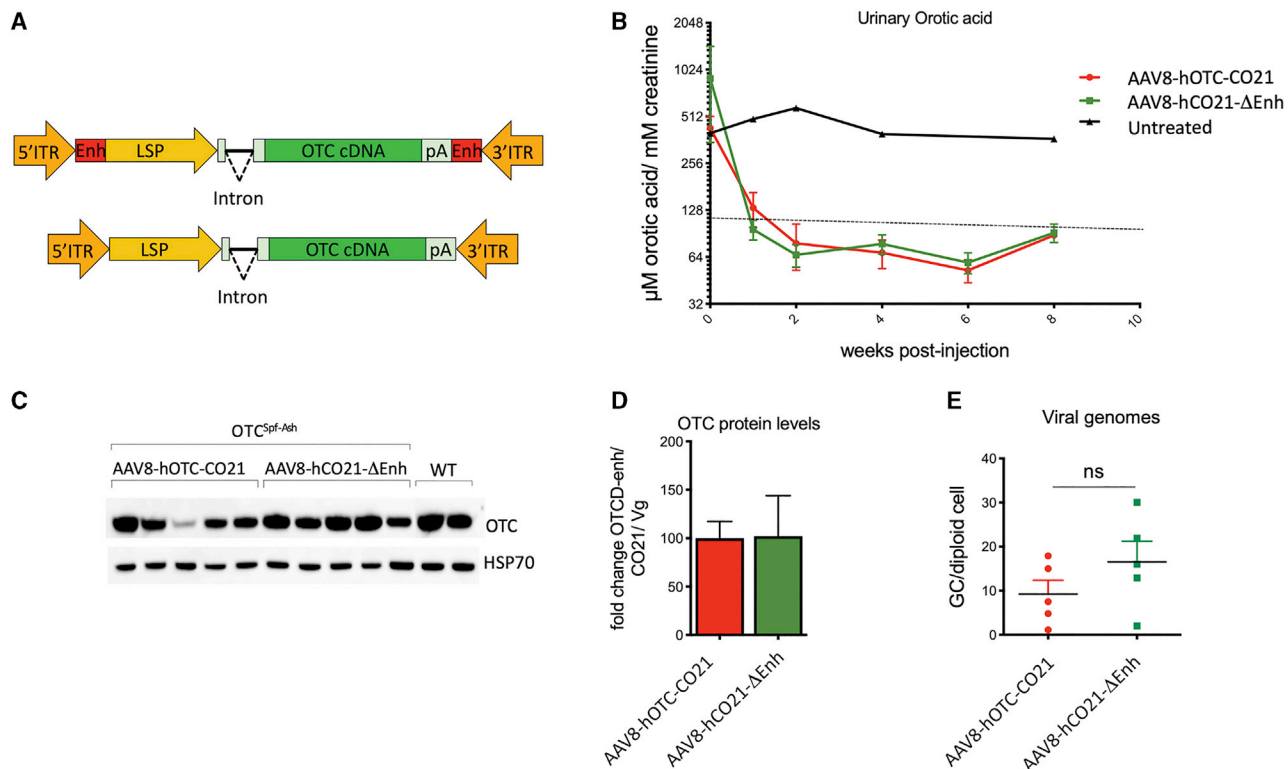


**Figure 5. Deletion of liver-specific enhancer sequences in the AAV vector backbone does not affect therapeutic efficacy**

(A) The segments next to the AAV ITRs containing liver-specific transcription binding sites (Enh, indicated as red rectangles) were removed to generate the AAV8-hOTC-CO21ΔEnh vector (bottom). ITR, AAV2 inverted terminal repeat; intron, modified hemoglobin (*HBB2*) beta intron; LSP, liver-specific promoter (*ApoE/hAAT*, hybrid promoter containing *ApoE* enhancer and *hAAT* promoter); hOTC, WT or CO hOTC open reading frame (ORF); pA, hemoglobin beta (*HBB*) polyadenylation signal. (B) 3-month-old OTC<sup>Spf-Ash</sup> mice were i.v. injected with 5.0E11 vg/kg of AAV8-hOTC-CO21 or AAV8-hOTC-CO21ΔEnh (n = 5 per group). Animals were sacrificed 8 weeks after viral delivery. Urine samples were collected every 2 weeks post-injection and analyzed for orotic acid levels. Orotic acid values were standardized against creatinine levels. Dashed line delimits physiological level of orotic acid. (C) OTC protein levels were determined by WB analysis. (D) Densitometric quantification of the WB of (C), normalized by the vg copy number. Data are shown as mean ± SEM. (E) The vg particles were determined by quantitative real-time PCR, and the mean values of two independent determinations are indicated. Data are shown as mean ± SEM, and statistical analyses were performed by unpaired *t* test (\**p* < 0.05).

To generate a highly expressed hOTC cDNA we used a combined strategy: initially, a series of CO OTC cDNAs were generated using different codon-optimization algorithms and evaluated for expression *in vitro* and *in vivo*. Next, the conserved domains and active sites of the most active constructs were shuffled to achieve an optimally expressed sequence, without altering the native amino acid sequence of the human enzyme. The conserved regions were identified by performing an alignment of OTC amino acid sequences of 142 species (Figure S2).<sup>28,29</sup> The shuffling of the conserved regions of the CO sequences generated an OTC cDNA, hOTC-CO21, that outperformed all previously tested hOTC CO versions. The optimized AAV8-hOTC-CO21 vector provided protein production and enzymatic activity up to 5- to 6-fold higher compared to those obtained with the WT hOTC cDNA, in both *in vitro* and *in vivo* experiments.

Using conventional algorithms, Wang et al.<sup>18</sup> also reported highly expressed CO hOTC cDNA versions under the control of the thyroxine-binding globulin (*TBG*) gene promoter. We created a

construct, hOTC-CO1, with the CO sequence described by Wang et al.<sup>18</sup> using the same promoter and other cassette elements as those used in AAV-hOTC-CO21. A side-by-side analysis showed increased protein production and enzymatic activity in the animals treated with the AAV vector expressing the hOTC-CO21 cDNA, compared to those expressing the hOTC-CO1 cDNA.

The AAV8-hOTC-CO21ΔEnhancer gene-therapy vector presented here allowed the complete and long-term correction of the phenotype present in OTC<sup>Spf-Ash</sup> mice at a relatively low dose. Our data demonstrated that the 5.0E11 vg/kg dose was able to robustly restore WT levels of liver OTC expression and activity, normalizing urinary orotic acid levels, the main biomarker of OTCD.<sup>6</sup> Importantly, this dose completely restored the urea cycle, with normalization of behavioral parameters and clinical protection during an acute ammonia challenge, similar to those observed in WT animals. This test has particular relevance, since a bolus of ammonia, the main neurotoxic metabolite that accumulates upon dysfunction of the urea cycle,<sup>34</sup> is given to the animals, and the OTC absence or its reduced activity results in immediate serious dysfunctions

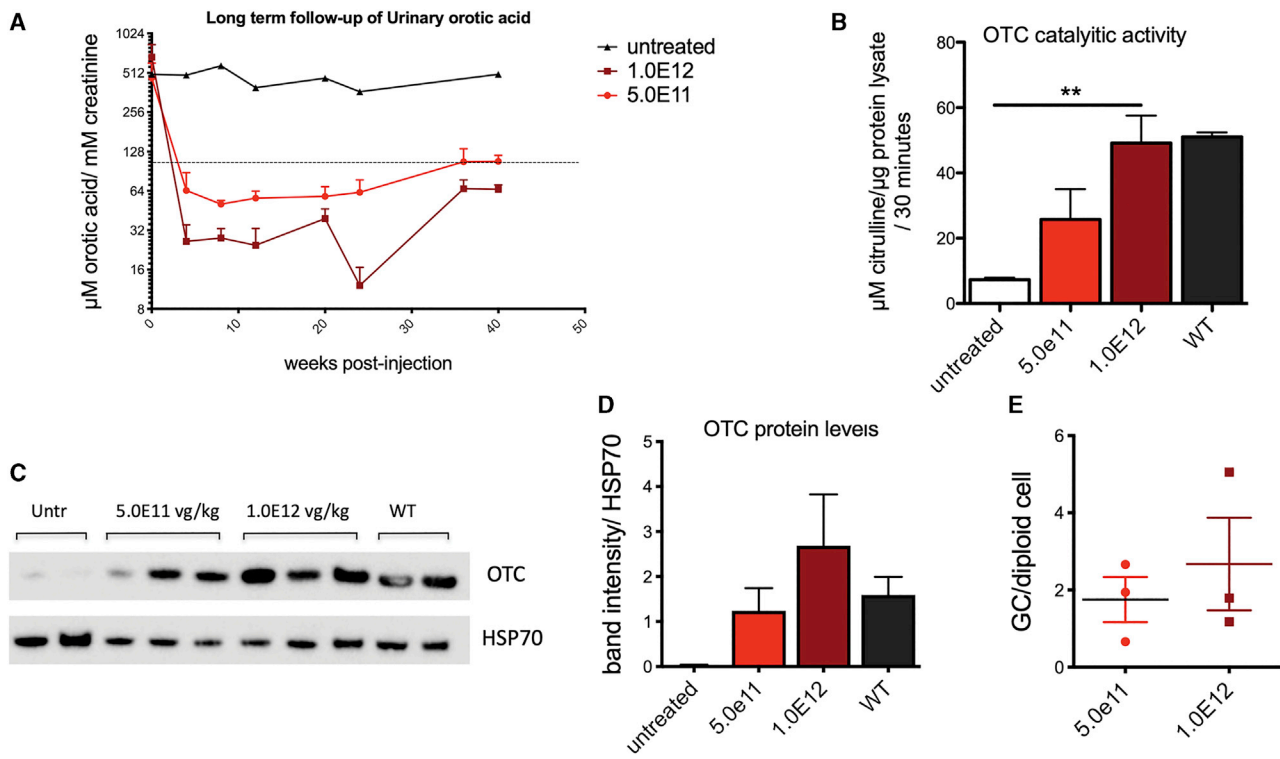


**Figure 6. Long-term evaluation of hOTC-CO21 transgene expression in adult *OTC<sup>Spf-Ash</sup>* mice**

12-week-old mice were i.v. injected with 5.0E11 vg/kg or 1.0E12 vg/kg of the AAV8-hOTC-CO21 or AAV8-hOTC-CO21 $\Delta$ Enh constructs (n = 4). Animals were sacrificed 40 weeks after viral delivery. (A) Urine samples were collected every 2 weeks post-injection and analyzed for orotic acid levels. Orotic acid values were standardized against creatinine levels. Dashed line delimits physiological level of orotic acid. (B) OTC enzyme activity expressed in  $\mu$ mol of citrulline produced in 30 min of reaction. Data are shown as mean  $\pm$  SEM, and statistical analyses were performed by one-way ANOVA with Turkey's multiple comparison test (\*\*p < 0.05). (C) OTC protein levels were determined by WB analysis. HSP70 was used to normalize for protein load. Untr, untreated *OTC<sup>Spf-Ash</sup>* mice. (D) Densitometric quantification of the WB of (C). WT, untreated wild-type control animals. Data are shown as mean  $\pm$  SEM, and statistical analyses were performed by one-way ANOVA with Turkey's multiple comparison test. (E) The vg particles were determined by quantitative real-time PCR, and the mean values of two independent determinations are indicated. Data are shown as mean  $\pm$  SEM, and statistical analyses were performed by unpaired t test. (\*p < 0.05).

or death.<sup>18,33</sup> Importantly, the improvements in the therapeutic vector described here would allow for an important decrease in the therapeutic dose, thus reducing its genotoxic potential<sup>19</sup> and, consequently, increasing the overall safety of the approach. OTC expression levels correlated with catalytic activity, suggesting that the expressed exogenous protein was fully active in the hepatocytes. Moreover, we verified the correct subcellular localization of the OTC protein produced by the therapeutic vector, demonstrating that it is efficiently processed and translocated to mitochondria.

One of the potential safety concerns is genotoxicity of the AAV vector. In spite of being episomal vectors, preclinical studies have shown that a minor proportion of the viral AAV genomes may be randomly inserted into the host genome<sup>35,36</sup> with the risk of insertional mutagenesis and transactivation of nearby genes.<sup>21,22,37</sup> Factors such as the total vector dose and the promoter choice may affect the genotoxicity risk of AAV vectors.<sup>19</sup> In effect, the presence of the chicken  $\beta$ -actin (*CBA*) promoter or the liver-specific *TBG* promoter, commonly used in AAV vectors, results in the development of HCC when delivered in

neonate mice at doses of 1–2E11 vg/pup. Here, we have endeavored to minimize the genotoxicity potential of the therapeutic vector by selecting the hAAT promoter containing the *ApoE* enhancer,<sup>25</sup> which was not associated with hepatocellular cancers,<sup>19</sup> and a CO transgene sequence that allows for lower doses of vector. Additionally, sequences flanking the WT AAV ITRs have been found integrated in known cancer driver genes in patients with HCC.<sup>20</sup> Importantly, preclinical studies suggest that these sequences contain liver-specific TFBSs, promoting transcription of nearby genes,<sup>24</sup> with the risk of tumorigenesis.<sup>20–22,37</sup> Thus, to further mitigate the potential risk of hepatocarcinogenicity, we removed these transcriptional activator regions present in the AAV backbone. Deletion of these sequences did not affect gene expression and the therapeutic potential of our vector, suggesting that their role in transcription is dispensable in the presence of a strong LSP. Importantly, treatment with the AAV8-hOTC-CO21 $\Delta$ Enhancer gene therapy did not result in liver damage or tumorigenesis, although further experimentation at higher vector doses and longer time may be needed to conclusively show the improved vector safety properties.



Thus, the results presented here further support the safe use of the AAV8-hOTC-CO21ΔEnhancer gene-therapy vector in clinical trials of OTCD patients. A clinical trial of AAV gene transfer for OTCD is currently ongoing (ClinicalTrials.gov: NCT02991144). While results are not published, early data emerging from the study indicate that high vector doses (1.0E13 vg/kg) are needed to achieve full therapeutic efficacy, which are associated with increase in liver enzymes and require the use of prophylactic immunomodulation (<https://ir.ultragenyx.com/news-releases/news-release-details/ultragenyx-announces-positive-longer-term-results-first-three>). Thus, the development of highly optimized gene transfer vectors could reduce the therapeutic vector dose and help mitigate potential vector genotoxicity and immune-mediated toxicities in humans (reviewed in Verdera et al.<sup>38</sup>).

An appropriate timing for the application of gene therapy is crucial for reasons related to the characteristics of both the disease and the vector. OTCD may present acutely soon after birth, during childhood, or in adulthood. In the neonatal-onset form of OTCD, the liver suffers from an acute toxic injury resulting in liver necrosis and regeneration, a condition that may be unsuitable for effective episomal gene transfer with non-integrative vectors. The infantile-onset form of OTCD represents a larger cohort of severely affected patients with normal liver architecture and function and are potential candidates for AAV gene therapy.<sup>39</sup> However, the therapeutic approach may still require further improvements to be applied in the neonatal/infantile setting. In fact, gene therapy in this context will probably result in the gradual loss of AAV DNA during hepatocyte duplication and, consequently, loss of therapeutic efficacy during liver growth,<sup>16,40–42</sup> requiring re-administration of the therapeutic medical product. Currently, vector re-dosing is limited by the generation of high-titer anti-AAV neutralizing antibodies (Nab) that may block vector transduction.<sup>11,43–45</sup> Thus, novel approaches should be developed to allow AAV re-administration in this challenging disease. Different strategies are being studied, such as interfering with the immune response at the time of viral administration<sup>46–48</sup> or depleting the serum of the patient from Nab generated during the first AAV administration.<sup>49–51</sup> Recently, co-administration of AAV8 vectors with ImmTOR nanoparticles containing rapamycin have been shown to mitigate the formation of anti-AAV antibodies and enable vector re-dosing in mice and non-human primates.<sup>48</sup> However, these promising approaches still require validation in the clinic.

In conclusion, considering that safety and efficacy are main requirements of vector development, in this study we developed an efficient and safe therapeutic vector able to completely rescue the phenotype of adult OTC-deficient Spf-Ash mice at relatively low AAV doses. Long-term follow-up of treated animals demonstrated steady expression of hOTC in the mouse liver with complete normalization of the disease phenotype, supporting the potential translation of this gene-transfer strategy to patients affected by OTCD.

## MATERIALS AND METHODS

### AAV vector construction

The hOTC cDNA was inserted in the pSDMD rAAV vector previously described.<sup>25</sup> Transcription of the hOTC transgene was driven

by a hybrid promoter containing the *ApoE* enhancer and the *hAAT* promoter and terminated by the hemoglobin beta (*HBB*) polyadenylation signal. The coding region and the promoter are separated by a human hemoglobin beta-derived synthetic intron (*HBB2*) modified by removal of alternative open reading frames longer than 50 base pairs.<sup>25</sup> CO variants of the *OTC* cDNA were generated using different optimization algorithms (Genscript, IDT, JCat, GeneArt, DNA 2.0) and cloned into the pSDMD rAAV vector. DNA synthesis was performed by Genscript, USA. The potential cryptic splicing sites were detected using a splicing-specific software and were manually removed. Potential alternative ARFs longer than 50 bases located in the coding and non-coding strands were manually removed. The hOTC-CO18 and hOTC-CO21 cDNA variants were generated by shuffling the conserved regions and domains containing the active sites of the most active versions. The conserved regions were identified by the alignment of OTCases of 142 species. OTC sequences from a broad range of species from bacteria to human were obtained from the Uniprot databank (Table S1), aligned, and analyzed for sequence conservation using the Seq2Logo software (<http://www.cbs.dtu.dk/biotools/Seq2Logo/>). The AAV-hOTC-CO21ΔEnhancer vector is devoid of 2 sequences containing enhancing elements downstream of the 5' ITR (5'gtagtaatgattaaccgccatgctacttatctacgtagccatgct 3') and upstream of the 3' ITR (5'agcatggctacgtagataagtagcatggcgggtaataactaac 3').

### AAV vector production

Research-grade AAV vectors pseudo-serotyped with the AAV8 capsid proteins were produced according to a modified version of the adenovirus-free transient transfection methods as previously described<sup>52</sup> and purified by CsCl gradient centrifugation.<sup>53,54</sup>

Genome-containing AAV vectors and empty AAV capsid particles were titrated using a quantitative real-time polymerase chain reaction and confirmed by SDS-PAGE followed by SYPRO Ruby protein gel stain and band densitometry.

### Cell culture and transfection

Human Huh-7 cells were maintained in Dulbecco's modified 's medium (DMEM; Thermo Fisher Scientific, Gibco) supplemented with 10% fetal bovine serum and 1% antibiotic+antimycotic solution (Sigma-Aldrich). Huh-7 cells were transfected with AAV8-hOTC and pGFP-C2 plasmid using lipofectamine 2000 (Invitrogen) following the manufacturer's instructions.

### OTC immunostaining in Huh-7 cells

24 h after transfection, Huh-7 cells were incubated with the Mitotracker red FM (Thermo Fisher) probe following manufacturer's instructions. After 30 min of incubation, cells were washed with PBS and fixed for 10 min in formaldehyde solution (4%). After 3 consecutive washes with PBS, cells were incubated in blocking buffer (5% normal goat serum, 0.3% Triton-X, PBS) for 1 h. Rabbit anti-human OTC antibody from Abcam (Ab203859) was incubated for 2 h (dilution 1/100), followed by 1 h incubation with the secondary antibody (Alexa Fluor 488 goat anti-rabbit A11034). Cells were then analyzed by confocal microscopy.

### Mouse model and animal studies

All animal care and experimental procedures were evaluated and approved by the ICGEB board and the Italian Ministry of Health (Ministero Italiano della Salute, authorization no. 926/2017-PR), with the full respect to the EU directive 2010/63/EU.

Breeding pairs of OTC<sup>Spf-Ash</sup> mice (B6EiC3Sn a/A-OTC<sup>Spf-Ash</sup>/J) were purchased from Jackson Laboratories (stock no. 001811), and the colony was expanded and maintained in the ICGEB Bio experimentation facility. All injections were administered via the i.v. (tail vein) route at 8–16 weeks of age in male hemizygote OTC<sup>Spf-Ash</sup> mice.

### Western blot analysis

Cells were collected and lysed in lysis buffer (0.5% triton-X, 10 mM HEPES [pH 7.4], 2 mM DTT). 20 µg of total cellular lysates were separated on 4%–12% Bis-Tris NuPage gel (Invitrogen).

Livers were collected and reduced in powder using a mortar and liquid nitrogen. Total liver protein extracts were extracted with a homogenizer in lysis buffer. Proteins in total liver lysates (1 µg per lane for WT mouse lysates and 8 µg per lane for OTC<sup>Spf-Ash</sup> lysates) were separated on a 10% SDS gel or Precast 4%–10% SDS gel (Invitrogen).

Proteins were transferred onto a nitrocellulose membrane, blocked with Blok-CH reagent (Millipore), and probed with rabbit anti-human OTC antibody (Abcam, Ab203859; dilution 1/3,000) and anti-hsp70 antibody (dilution 1/8,000). The primary antibody was detected with a goat anti-rabbit immunoglobulin G-horseradish peroxidase (IgG-HRP) or anti-rat, respectively.

### OTC enzyme activity assay

OTC enzyme activity was determined in total liver protein extracts as reported previously,<sup>55</sup> with minor modifications. 1 µg of total liver protein extract (in lysis buffer) was added to 350 µL of reaction mixture (5 mM ornithine, 15 mM carbamyl phosphate, and 270 mM triethanolamine [pH 7.7]) and incubated at 37°C for 30 min. The reaction was then stopped by adding 125 µL of 3:1 phosphoric/sulfuric acid solution followed by 25 µL of 3% 2,3-butanedione monoxime and incubated at 95°C for 15 min in the dark. Citrulline production was determined by measuring the absorbance at 490 nm. The assays were performed in duplicate.

### Viral genome copy quantification in the liver

Genomic DNA was extracted from pulverized liver using the Wizard SV genomic DNA purification system (Promega) following the manufacturer's guidelines. Vector genomes in liver were quantified by real-time PCR using the iQ SYBER green supermix (Bio-Rad), using primers targeting inside the promoter region as previously described.<sup>40</sup>

### Urinary orotic acid determination

Urine was freshly collected before treatment (T0) and every 2 weeks or every month after the treatment and analyzed for orotic acid by high-performance liquid chromatography (HPLC)-tandem mass spectrometry, as described below.

Orotic acid was purchased from Sigma-Aldrich. The isotopically labeled internal standard orotic acid was purchased from Cambridge Isotope Laboratories.

The quantitative experiments were done using as internal standard the isotopically labeled 1,3-15N2 orotic acid in 200 µM concentration both for calibration curve and samples.

A typical calibration curve ranged from 15 µM to 300 µM with excellent linearity ( $R^2 > 0.99$ ). A Bruker (Bremen, Germany) amaZonSL bench-top ion trap mass spectrometer, equipped with an electrospray source, was employed for this study. The source was operated in negative-ion mode with a needle potential of 4,500 V and a gas flow of 12 L/min of nitrogen with heating at 200°C. The chromatographic separations for quantitative experiments were performed using a series 1260 Agilent Technologies (Waldbronn, Germany) HPLC with autosampler controlled from the Bruker Hystar data system. A Phenomenex (Torrance, USA) HPLC column Gemini C18 5 µm, 110Å, 2 × 150-mm was employed. Column flow rate was 0.4 mL/min, and elution was performed using 5 min wash time after 10-µL injection and a 3 min gradient from water with 0.1% formic acid to 90% acetonitrile with 0.1% formic acid. The tandem mass spectrometry (MS/MS) transitions used for the quantitative experiments (multiple reaction monitoring, MRM) were m/z 155.1 to 111.1 (orotic acid) and 157.1 to 113.1 (1,3-15N2 orotic acid). The acquired data were processed using the Bruker Compass Data Analysis proprietary software.

Creatinine was measured using the mouse creatinine kit (Crystal Chem, 80350) following the manufacturer's guidelines and used to normalize orotic acid values in the urine.

### Ammonia challenge

Ammonia challenge was performed on a dedicated group of mice at 4 and 8 weeks post-AAV treatment. After the second challenge, the mice were sacrificed and the livers were collected to analyze OTC enzymatic activity and vg. For the challenge, mice were injected intraperitoneally with a 0.75 M NH<sub>4</sub>Cl solution at the dose of 7.5 mmol/kg. Twenty minutes after the injection, mice were subjected to a behavioral test as previously described.<sup>15,17,32,33</sup> As described, the score was based on ataxia, response to sound, and seizure, using a scale from 0 to 3, with 3 indicating normal and 0 indicating the most severe impairment. The genotype of the animals and the treatment were unknown to the operator. Untreated OTC<sup>Spf-Ash</sup> and WT littermates were used as controls. Immediately after the behavioral test, urine was collected to analyze orotic acid, and a blood sample was collected by cheek puncture to analyze ammonia using the ammonia kit (Sigma AA0100) following the manufacturer's instructions.

### Transaminase determination

Transaminases were determined in serum using the ALT activity assay (Sigma-Aldrich, cat. no. MAK052) and the AST activity assay (Sigma-Aldrich, cat. no. MAK055) kits, following the manufacturer's instructions.

### Statistical analysis

Data are expressed as means  $\pm$  SD or mean  $\pm$  SEM, as indicated. Statistical analyses were performed with the GraphPad Prism package. Two-tailed unpaired Student's *t* test was performed to compare 2 groups; one-way ANOVA followed by the indicated post hoc tests were performed when comparing more than two groups. Two-way ANOVA followed by the indicated post hoc tests were performed when comparing more than two groups relative to two factors. A *p* value  $<0.05$  was considered statistically significant.

### SUPPLEMENTAL INFORMATION

Supplemental Information can be found online at <https://doi.org/10.1016/j.omtm.2020.11.005>.

### ACKNOWLEDGMENTS

The authors thank the ICGEB BioExperimentation Facility for help with animal care. This work was supported by ICGEB intramural funding to AFM and by Selecta Biosciences.

### AUTHOR CONTRIBUTIONS

A.F.M., T.K.K., P.I., L.D.A., and F.M. conceived the project and analyzed data; F.B., G.B., E.N., and P.I. analyzed data; G.D.S. performed most experiments and analyzed data; C.G. performed the orotic acid determination; A.I., F.C., G.R., M.S.S., P.V., J.R., and S.C. performed cloning and preparation of AAV stocks; A.F.M. and G.D.S. wrote the manuscript. All authors read and participated in the correction of the manuscript.

### DECLARATION OF INTERESTS

F.M. is currently an employee of Spark Therapeutics, a Roche company. P.I. and T.K.K. are employees of Selecta Biosciences.

### REFERENCES

- Gordon, N. (2003). Ornithine transcarbamylase deficiency: a urea cycle defect. *Eur. J. Paediatr. Neurol.* *7*, 115–121.
- Pampols, T. (2010). Inherited metabolic rare disease. *Adv. Exp. Med. Biol.* *686*, 397–431.
- Appelgarth, D.A., Toone, J.R., and Lowry, R.B. (2000). Incidence of inborn errors of metabolism in British Columbia, 1969–1996. *Pediatrics* *105*, e10.
- Summar, M.L., Koelker, S., Freedenberg, D., Le Mons, C., Haberle, J., Lee, H.-S., and Kirmse, B.; European Registry and Network for Intoxication Type Metabolic Diseases (E-IMD). Electronic address: <http://www.e-imd.org/en/index.phtml>; Members of the Urea Cycle Disorders Consortium (UCDC). Electronic address: <http://rarediseases-network.epi.usf.edu/ucdc/> (2013). The incidence of urea cycle disorders. *Mol. Genet. Metab.* *110*, 179–180.
- Brusilow, S.W., and Maestri, N.E. (1996). Urea cycle disorders: diagnosis, pathophysiology, and therapy. *Adv. Pediatr.* *43*, 127–170.
- Häberle, J., Bodaert, N., Burlina, A., Chakrapani, A., Dixon, M., Huemer, M., Karall, D., Martinelli, D., Crespo, P.S., Santer, R., et al. (2012). Suggested guidelines for the diagnosis and management of urea cycle disorders. *Orphanet J. Rare Dis.* *7*, 32.
- Enns, G.M., Berry, S.A., Berry, G.T., Rhead, W.J., Brusilow, S.W., and Hamosh, A. (2007). Survival after treatment with phenylacetate and benzoate for urea-cycle disorders. *N. Engl. J. Med.* *356*, 2282–2292.
- Adam, R., Karam, V., Delvar, V., O'Grady, J., Mirza, D., Klemppauer, J., Castaing, D., Neuhaus, P., Jamieson, N., Salizzoni, M., et al.; All contributing centers ([www.eltr.org](http://www.eltr.org)); European Liver and Intestine Transplant Association (ELITA) (2012). Evolution of indications and results of liver transplantation in Europe. A report from the European Liver Transplant Registry (ELTR). *J. Hepatol.* *57*, 675–688.
- Neuberger, J. (2016). An update on liver transplantation: A critical review. *J. Autoimmun.* *66*, 51–59.
- Herrero, J.I. (2009). De novo malignancies following liver transplantation: impact and recommendations. *Liver Transpl.* *15* (Suppl 2), S90–S94.
- Nathwani, A.C., Reiss, U.M., Tuddenham, E.G., Rosales, C., Chowdary, P., McIntosh, J., Della Peruta, M., Lheriteau, E., Patel, N., Raj, D., et al. (2014). Long-term safety and efficacy of factor IX gene therapy in hemophilia B. *N. Engl. J. Med.* *371*, 1994–2004.
- Nathwani, A.C., Tuddenham, E.G., Rangarajan, S., Rosales, C., McIntosh, J., Linch, D.C., Chowdary, P., Riddell, A., Pie, A.J., Harrington, C., et al. (2011). Adenovirus-associated virus vector-mediated gene transfer in hemophilia B. *N. Engl. J. Med.* *365*, 2357–2365.
- Rangarajan, S., Walsh, L., Lester, W., Perry, D., Madan, B., Laffan, M., Yu, H., Vettermann, C., Pierce, G.F., Wong, W.Y., and Pasi, K.J. (2017). AAV5-Factor VIII Gene Transfer in Severe Hemophilia A. *N. Engl. J. Med.* *377*, 2519–2530.
- George, L.A., Sullivan, S.K., Giermasz, A., Rasko, J.E.J., Samelson-Jones, B.J., Ducore, J., Cuker, A., Sullivan, L.M., Majumdar, S., Teitel, J., et al. (2017). Hemophilia B Gene Therapy with a High-Specific-Activity Factor IX Variant. *N. Engl. J. Med.* *377*, 2215–2227.
- Moscioni, D., Morizono, H., McCarter, R.J., Stern, A., Cabrera-Luque, J., Hoang, A., Sanmiguel, J., Wu, D., Bell, P., Gao, G.P., et al. (2006). Long-term correction of ammonia metabolism and prolonged survival in ornithine transcarbamylase-deficient mice following liver-directed treatment with adeno-associated viral vectors. *Mol. Ther.* *14*, 25–33.
- Cunningham, S.C., Spinoulas, A., Carpenter, K.H., Wilcken, B., Kuchel, P.W., and Alexander, I.E. (2009). AAV2/8-mediated correction of OTC deficiency is robust in adult but not neonatal Spf(ash) mice. *Mol. Ther.* *17*, 1340–1346.
- Wang, L., Wang, H., Morizono, H., Bell, P., Jones, D., Lin, J., McMenamin, D., Yu, H., Batshaw, M.L., and Wilson, J.M. (2012). Sustained correction of OTC deficiency in spf(ash) mice using optimized self-complementary AAV2/8 vectors. *Gene Ther.* *19*, 404–410.
- Wang, L., Morizono, H., Lin, J., Bell, P., Jones, D., McMenamin, D., Yu, H., Batshaw, M.L., and Wilson, J.M. (2012). Preclinical evaluation of a clinical candidate AAV8 vector for ornithine transcarbamylase (OTC) deficiency reveals functional enzyme from each persisting vector genome. *Mol. Genet. Metab.* *105*, 203–211.
- Chandler, R.J., LaFave, M.C., Varshney, G.K., Trivedi, N.S., Carrillo-Carrasco, N., Senac, J.S., Wu, W., Hoffmann, V., Elkhoulou, A.G., Burgess, S.M., and Venditti, C.P. (2015). Vector design influences hepatic genotoxicity after adeno-associated virus gene therapy. *J. Clin. Invest.* *125*, 870–880.
- Nault, J.-C., Mami, I., La Bella, T., Datta, S., Imbeaud, S., Franconi, A., Mallet, M., Couchy, G., Letouze, E., Pilati, C., et al. (2016). Wild-type AAV Insertions in Hepatocellular Carcinoma Do Not Inform Debate Over Genotoxicity Risk of Vectorized AAV. *Mol. Ther.* *24*, 660–661.
- Donsante, A., Miller, D.G., Li, Y., Vogler, C., Brunt, E.M., Russell, D.W., and Sands, M.S. (2007). AAV vector integration sites in mouse hepatocellular carcinoma. *Science* *317*, 477.
- Donsante, A., Vogler, C., Muzyczka, N., Crawford, J.M., Barker, J., Flotte, T., Campbell-Thompson, M., Daly, T., and Sands, M.S. (2001). Observed incidence of tumorigenesis in long-term rodent studies of rAAV vectors. *Gene Ther.* *8*, 1343–1346.
- La Bella, T., Imbeaud, S., Peneau, C., Mami, I., Datta, S., Bayard, Q., Caruso, S., Hirsch, T.Z., Calderaro, J., Morcrette, G., et al. (2020). Adeno-associated virus in the liver: natural history and consequences in tumour development. *Gut* *69*, 737–747.
- Logan, G.J., Dane, A.P., Hallwirth, C.V., Smyth, C.M., Wilkie, E.E., Amaya, A.K., Zhu, E., Khandekar, N., Ginn, S.L., Liao, S.H.Y., et al. (2017). Identification of liver-specific enhancer-promoter activity in the 3' untranslated region of the wild-type AAV2 genome. *Nat. Genet.* *49*, 1267–1273.
- Ronzitti, G., Bortolussi, G., van Dijk, R., Collaud, F., Charles, S., Leborgne, C., Vidal, P., Martin, S., Gjata, B., Sola, M.S., et al. (2016). A translationally optimized AAV-UGT1A1 vector drives safe and long-lasting correction of Crigler-Najjar syndrome. *Mol. Ther. Methods Clin. Dev.* *3*, 16049.

26. Wang, L., Bell, P., Morizono, H., He, Z., Pumbo, E., Yu, H., White, J., Batshaw, M.L., and Wilson, J.M. (2017). AAV gene therapy corrects OTC deficiency and prevents liver fibrosis in aged OTC-knock out heterozygous mice. *Mol. Genet. Metab.* *120*, 299–305.
27. Li, C., Goudy, K., Hirsch, M., Asokan, A., Fan, Y., Alexander, J., Sun, J., Monahan, P., Seiber, D., Sidney, J., et al. (2009). Cellular immune response to cryptic epitopes during therapeutic gene transfer. *Proc. Natl. Acad. Sci. USA* *106*, 10770–10774.
28. Shi, D., Morizono, H., Ha, Y., Aoyagi, M., Tuchman, M., and Allewell, N.M. (1998). 1.85-Å resolution crystal structure of human ornithine transcarbamoylase complexed with N-phosphonacetyl-L-ornithine. Catalytic mechanism and correlation with inherited deficiency. *J. Biol. Chem.* *273*, 34247–34254.
29. Shi, D., Morizono, H., Yu, X., Tong, L., Allewell, N.M., and Tuchman, M. (2001). Human ornithine transcarbamoylase: crystallographic insights into substrate recognition and conformational changes. *Biochem. J.* *354*, 501–509.
30. DeMars, R., LeVan, S.L., Trend, B.L., and Russell, L.B. (1976). Abnormal ornithine carbamoyltransferase in mice having the sparse-fur mutation. *Proc. Natl. Acad. Sci. USA* *73*, 1693–1697.
31. Hodges, P.E., and Rosenberg, L.E. (1989). The spfash mouse: a missense mutation in the ornithine transcarbamoylase gene also causes aberrant mRNA splicing. *Proc. Natl. Acad. Sci. USA* *86*, 4142–4146.
32. Crawley, J.N. (2007). What's Wrong With My Mouse?: Behavioral Phenotyping of Transgenic and Knockout Mice (Wiley).
33. Ye, X., Robinson, M.B., Pabin, C., Quinn, T., Jawad, A., Wilson, J.M., and Batshaw, M.L. (1997). Adenovirus-mediated in vivo gene transfer rapidly protects ornithine transcarbamoylase-deficient mice from an ammonium challenge. *Pediatr. Res.* *41*, 527–534.
34. Campbell, A.G., Rosenberg, L.E., Snodgrass, P.J., and Nuzum, C.T. (1973). Ornithine transcarbamoylase deficiency: a cause of lethal neonatal hyperammonemia in males. *N. Engl. J. Med.* *288*, 1–6.
35. McCarty, D.M., Young, S.M., Jr., and Samulski, R.J. (2004). Integration of adeno-associated virus (AAV) and recombinant AAV vectors. *Annu. Rev. Genet.* *38*, 819–845.
36. Russell, D.W., Miller, A.D., and Alexander, I.E. (1994). Adeno-associated virus vectors preferentially transduce cells in S phase. *Proc. Natl. Acad. Sci. USA* *91*, 8915–8919.
37. Chandler, R.J., Sands, M.S., and Venditti, C.P. (2017). Recombinant Adeno-Associated Viral Integration and Genotoxicity: Insights from Animal Models. *Hum. Gene Ther.* *28*, 314–322.
38. Verdera, H.C., Kuranda, K., and Mingozzi, F. (2020). AAV Vector Immunogenicity in Humans: A Long Journey to Successful Gene Transfer. *Mol. Ther.* *28*, 723–746.
39. Muro, A.F., D'Antiga, L., and Mingozzi, F. (2018). Gene therapy in pediatric liver disease. In *Pediatric Hepatology and Liver Transplantation*, L. D'Antiga, ed. (Springer), pp. 799–829.
40. Bortolussi, G., Zentilin, L., Vaníkova, J., Bockor, L., Bellarosa, C., Mancarella, A., Vianello, E., Tiribelli, C., Giacca, M., Vitek, L., and Muro, A.F. (2014). Life-long correction of hyperbilirubinemia with a neonatal liver-specific AAV-mediated gene transfer in a lethal mouse model of Crigler-Najjar Syndrome. *Hum. Gene Ther.* *25*, 844–855.
41. Cunningham, S.C., Dane, A.P., Spinoulas, A., Logan, G.J., and Alexander, I.E. (2008). Gene delivery to the juvenile mouse liver using AAV2/8 vectors. *Mol. Ther.* *16*, 1081–1088.
42. Wang, L., Wang, H., Bell, P., McMenamin, D., and Wilson, J.M. (2012). Hepatic gene transfer in neonatal mice by adeno-associated virus serotype 8 vector. *Hum. Gene Ther.* *23*, 533–539.
43. Mingozzi, F., and High, K.A. (2017). Overcoming the Host Immune Response to Adeno-Associated Virus Gene Delivery Vectors: The Race Between Clearance, Tolerance, Neutralization, and Escape. *Annu. Rev. Virol.* *4*, 511–534.
44. Ronzitti, G., Gross, D.A., and Mingozzi, F. (2020). Human Immune Responses to Adeno-Associated Virus (AAV) Vectors. *Front. Immunol.* *11*, 670.
45. Murphy, S.L., Li, H., Mingozzi, F., Sabatino, D.E., Hui, D.J., Edmonson, S.A., and High, K.A. (2009). Diverse IgG subclass responses to adeno-associated virus infection and vector administration. *J. Med. Virol.* *81*, 65–74.
46. Kishimoto, T.K., Ferrari, J.D., LaMothe, R.A., Kolte, P.N., Griset, A.P., O'Neil, C., Chan, V., Browning, E., Chalisehar, A., Kuhlman, W., et al. (2016). Improving the efficacy and safety of biologic drugs with tolerogenic nanoparticles. *Nat. Nanotechnol.* *11*, 890–899.
47. Maldonado, R.A., LaMothe, R.A., Ferrari, J.D., Zhang, A.H., Rossi, R.J., Kolte, P.N., Griset, A.P., O'Neil, C., Altreuter, D.H., Browning, E., et al. (2015). Polymeric synthetic nanoparticles for the induction of antigen-specific immunological tolerance. *Proc. Natl. Acad. Sci. USA* *112*, E156–E165.
48. Meliani, A., Boisgerault, F., Harget, R., Marmier, S., Collaud, F., Ronzitti, G., Leborgne, C., Costa Verdera, H., Simon Sola, M., Charles, S., et al. (2018). Antigen-selective modulation of AAV immunogenicity with tolerogenic rapamycin nanoparticles enables successful vector re-administration. *Nat. Commun.* *9*, 4098.
49. Leborgne, C., Barbon, E., Alexander, J.M., Hanby, H., Delignat, S., Cohen, D.M., Collaud, F., Muralettharan, S., Lupo, D., Silverberg, J., et al. (2020). IgG-cleaving endopeptidase enables in vivo gene therapy in the presence of anti-AAV neutralizing antibodies. *Nat. Med.* *26*, 1096–1101.
50. Bertin, B., Veron, P., Leborgne, C., Deschamps, J.Y., Moullec, S., Fromes, Y., Collaud, F., Boutin, S., Latournerie, V., van Wittenbergh, L., et al. (2020). Capsid-specific removal of circulating antibodies to adeno-associated virus vectors. *Sci. Rep.* *10*, 864.
51. Chicoine, L.G., Montgomery, C.L., Bremer, W.G., Shontz, K.M., Griffin, D.A., Heller, K.N., Lewis, S., Malik, V., Grose, W.E., Shilling, C.J., et al. (2014). Plasmapheresis eliminates the negative impact of AAV antibodies on microdystrophin gene expression following vascular delivery. *Mol. Ther.* *22*, 338–347.
52. Collaud, F., Bortolussi, G., Guianvarc'h, L., Aronson, S.J., Bordet, T., Veron, P., Charles, S., Vidal, P., Sola, M.S., Rundwasser, S., et al. (2018). Preclinical Development of an AAV8-hUGT1A1 Vector for the Treatment of Crigler-Najjar Syndrome. *Mol. Ther. Methods Clin. Dev.* *12*, 157–174.
53. Ayuso, E., Mingozzi, F., Montane, J., Leon, X., Anguela, X.M., Haurigot, V., Edmonson, S.A., Africa, L., Zhou, S., High, K.A., et al. (2010). High AAV vector purity results in serotype- and tissue-independent enhancement of transduction efficiency. *Gene Ther.* *17*, 503–510.
54. Matsushita, T., Elliger, S., Elliger, C., Podsakoff, G., Villarreal, L., Kurtzman, G.J., Iwaki, Y., and Colosi, P. (1998). Adeno-associated virus vectors can be efficiently produced without helper virus. *Gene Ther.* *5*, 938–945.
55. Ye, X., Robinson, M.B., Batshaw, M.L., Furth, E.E., Smith, I., and Wilson, J.M. (1996). Prolonged metabolic correction in adult ornithine transcarbamoylase-deficient mice with adenoviral vectors. *J. Biol. Chem.* *271*, 3639–3646.